Selective Tuning of a Particular Chemical Reaction on Surfaces Through Electrical Resonance: An Ab Initio Molecular Dynamics Study

ARTICLE *in* JOURNAL OF PHYSICAL CHEMISTRY LETTERS · DECEMBER 2015

Impact Factor: 7.46 · DOI: 10.1021/acs.jpclett.5b02420

THE JOURNAL OF PHYSICAL CHEMISTRY Letters

Letter

pubs.acs.org/JPCL

Selective Tuning of a Particular Chemical Reaction on Surfaces through Electrical Resonance: An ab Initio Molecular Dynamics Study

Masood Yousaf,[†] Dongbin Shin,[‡] Rodney Ruoff,[†,§] and Noejung Park*[,†,‡]

[†]IBS Center for Multidimensional Carbon Materials, [‡]Department of Physics, and [§]Department of Chemistry, Ulsan National Institute of Science and Technology, Ulsan, 689-798 Korea

Supporting Information

ABSTRACT: We used ab initio molecular dynamics (AIMD) to investigate the effect of a monochromatic oscillating electric field in resonance with a particular molecular vibration on surfaces. As a case study, AIMD simulations were carried out for hydroxyl functional groups on graphene. When the frequency of the applied field matches with the C−OH vibration frequency, the amplitude is monotonically amplified, leading to a complete desorption from the surface, overcoming the substantial barrier. This suggests the possibility of activating a particular bond without damaging the remaining surface. We extended this work to the case of the amination of sp^2-bonded carbon surfaces and discussed the general perspective that, in general, an unfavorable chemical process can be activated by applying an external electric field with an appropriate resonance frequency.

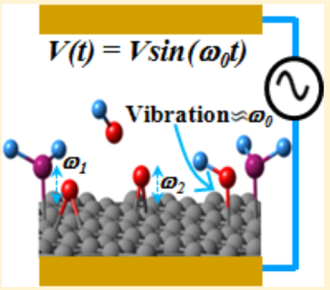

As the fabrication of nanomaterials flourishes in many research areas, the properties of surfaces have become more important,[1] and techniques for the treatment of surfaces are attracting increasing attention to achieve the desired material property.[2−4] Over the years, various types of physical and chemical methods have been developed, and their strengths and weaknesses have been widely discussed elsewhere.[5−8] Physical methods such as ultraviolet (UV) radiation[9] and plasma treatment[10] often produce ill-defined and defective surfaces.[11] The plasma surface modification technique is, in general, expensive and requires a high density of active ions and specialized equipment such as plasma reactors.[12,13] Chemical heat treatment takes a longer processing time and has a significant risk of deforming the material.[14] All these methods are not really suitable for modifying the atomic details of specific functional groups on the surface. Because adsorption or desorption of a particular functional group has a profound effect on inter- and intrasurface interactions, a more sophisticated method targeting a particular functional group is necessary.

In this work, we investigate the effect of an oscillating electric field (E-field) in resonance with the vibration of a particular functional group on a surface. Scheme 1 describes our motivation. A synthesis process might have left behind unwanted functional groups, such as hydroxyl (OH), on the grown graphene surface, and a postsynthesis treatment which can remove them without damaging the remaining part is desirable. This study examines whether an E-field whose frequency matches the natural vibrational frequency of the functional group can serve such a purpose. As shown in Scheme 1, an external electric potential with the same frequency as the C−O bond is applied perpendicular to the OH-adsorbed on the graphene surface. As will be shown later, the C−O bond can be selectively activated under the resonating E-field, finally leading to its detachment.

Scheme 1. Schematic of the Proposed Surface Modification Method[a]

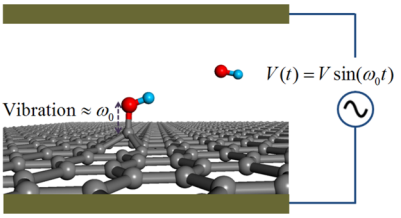

[a]An external electric field is applied with the same oscillating frequency as the vibration frequency of a particular bond.

As a case study, we focus on functional groups on graphene which may serve as an atomistic model for graphene oxide (GO). We calculated the vibration frequency of a specific adsorption structure and traced its response to an applied oscillating electric bias with the same frequency. We are mainly interested in the response of a functional group on the surface when the applied field has the same frequency as the vibration of a particular bond. As an example (Figure 1), we selected a system with an adsorbed OH on graphene, and an external electric potential, with the same frequency as the vibration frequency of a C−O bond, was applied perpendicular to the surface. The C−O vibration is embedded in several phonon modes of the OH-adsorbed graphene and can hardly be singled out. To extract the most relevant frequency, we traced the vibration of C−O in real time with various initial conditions. As will be shown later, the resonating E-field causes a monotonous increase in the amplitude, leading to the breaking of the C−O

Received: October 29, 2015
Accepted: December 4, 2015

DOI: 10.1021/acs.jpclett.5b02420
J. Phys. Chem. Lett. 2015, 6, 5094−5099

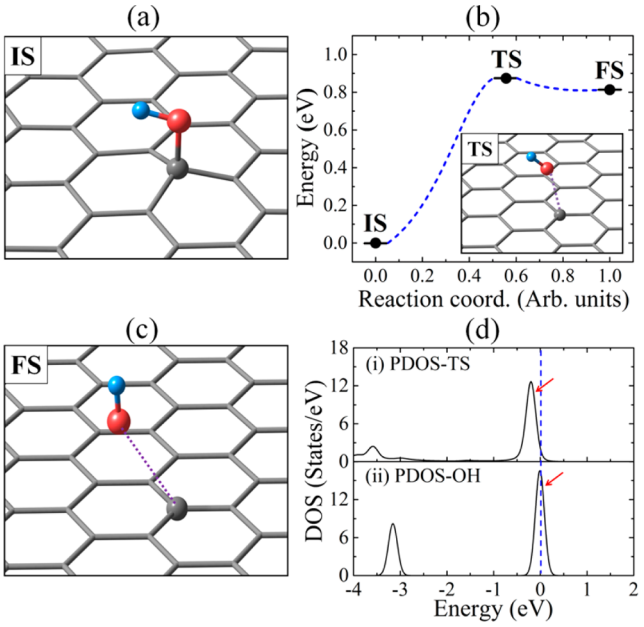

Figure 1. (a) Initial state (IS) configuration for the OH-adsorbed graphene. (b) Potential energy curve for the desorption of OH from graphene. (c) Final state (FS) configuration in which OH is desorbed. The inset in panel b shows the transition state (TS) configuration in which the C−O bond length is 2.52 Å. (d) Projected density of electronic states for OH (i) in the TS configuration and (ii) in the isolated neutral OH in vacuum. Small sky blue and red balls indicate H and O atoms, respectively. The C atom on which OH was bonded is denoted by a gray ball, while the other C atoms in graphene are represented by only the wire frame.

bond. This method can be applied to the removal of unwanted functional groups. It is to be noted that we adopted a simple and clear approach to describe and implement our proposed modification method.

The proposed method can lead to a general surface treatment technique that is potentially capable of tailoring the atomic details of surface functional groups. Contaminants can be removed by choosing the frequency of the applied E-field, and as a result, the surface can be effectively grafted with a certain functional group to develop a specific character.[15] Compared with the aforementioned bulk treatment techniques, the surface-resonating E-field is expected to have a negligible effect on the bulk or substrate.[16] This technique is not only for the purpose of surface cleaning; it can be extended to the promotion of a particular chemical reaction by exciting relevant bonds in the reaction, which is otherwise almost forbidden because of limited kinetic paths. A controlled growth of particular reactive species on the surfaces can be used for catalytic functions of surfaces, or even to enhance the performance of medical implants in a biological environment. The proposed method can receive a great boost from the development of computational methods. For example, density functional theory (DFT) has provided an affordable computation method for the quantum mechanical properties of various materials. Even though DFT, as an effective one-body theory for a many-electron system, may not have a perfect transferability for an arbitrary system, it is important to note that the vibration frequency can be accurately calculated from the second derivative of the total energy. The frequency of an expected adsorption structure can be calculated, providing input for the required resonating field in an experimental setup.

Born−Oppenheimer ab initio molecular dynamics (AIMD) simulations and other DFT calculations were performed using the Quantum ESPRESSO code,[17] which utilizes plane wave basis sets and pseudopotentials. For the DFT calculations, the Perdew and Wang (PW) type exchange-correlation potential was used.[18] Norm-conserving pseudopotentials[19] generated by the Martins−Troullier method[20] were used for the atomic potentials of H, C, N, and O. A plane wave basis set with a 60 Ry energy cutoff was used to describe wave functions. Integrals over the Brillouin zone were evaluated using 9 × 9 × 1 Monkhorst−Pack k-point mesh for geometry optimization and 60 × 60 × 1 for the calculation of charge transfer and density of states. The nudged elastic band (NEB)[21,22] method, as implemented in the Quantum ESPRESSO code, was used to calculate the minimum energy path (MEP) along with the transition energies. To apply the E-field over the super cell, we used a sawtooth-type potential along the specified direction. For the oscillating electric field in AIMD simulations, the electric potential was implemented as $V_{ext}(\vec{r}, t) = V_0(z)\sin(\omega t)$. Molecular dynamics was performed through the forces calculated by the derivative of the following total energy functional.

$$E_{tot} = E^{DFT}[\rho(\vec{r}, t), \vec{R}_\lambda] + \int \rho(\vec{r}, t)\, V_{ext}(\vec{r}, t)\, d^3\vec{r} - \sum_\lambda \int Z_\lambda \delta(\vec{r} - \vec{R}_\lambda)\, V_{ext}(\vec{r}, t)\, d^3\vec{r}$$

$$\vec{F}_\lambda = -\frac{\partial E^{DFT}[\rho(\vec{r}, t), \vec{R}_\lambda]}{\partial \vec{R}_\lambda} + Z_\lambda \vec{E}_0 \sin(\omega t)$$

where Z_λ is the pseudo atomic number and $\vec{E}_0$ indicates uniform e-field which corresponds to $-\nabla V_0$. The time-dependent electron density, which evolves along the Born−Oppenheimer potential energy surface, comprised the DFT functional. Thus, the atomic forces consist of the gradient of the total energy functional and the electrostatic force acting on the point charge of atom core. The time step of 20 a.u (0.968 fs) was used in the integration of AIMD steps. Two E-field intensities of 0.05 V/Å and 0.025 V/Å were used, which correspond to laser intensity of 3.32×10^{10} W/cm^2 and 8.30×10^9 W/cm^2, which is largely in the range of that of the laser pulse used in experiments.[23]

We first investigate the potential energy surface for the desorption path of OH from graphene without external electric field. The optimized geometries of the initial adsorbed state (IS), transition state (TS), and final desorbed state (FS) configurations are presented in panel a, the inset of panel b, and panel c in Figure 1, respectively. The energy profile during desorption process is summarized in Figure 1b. The distances between the O atom of the OH and the C atom of graphene on which OH is bonded are 1.47, 2.52, and 2.86 Å for the IS, TS, and FS states, respectively. The upper (i) and lower (ii) sections of Figure 1d show the projected density of states (PDOS) of OH on the graphene surface for the TS configuration and for an isolated OH in vacuum, respectively. The Fermi level is set at 0.0 eV, indicated by a blue vertical dashed line. The peaks at the Fermi level, indicated by arrows in Figure 1d, are the doubly degenerate nonbonding orbitals of OH. In the PDOS for TS, the peak is located slightly below the Fermi level, indicating a fractional charge transfer from graphene to OH. Bader charge analysis revealed a consistent result.[24] Bader charges of +1 and −1 appear on H and O,

DOI: 10.1021/acs.jpclett.5b02420
J. Phys. Chem. Lett. 2015, 6, 5094−5099

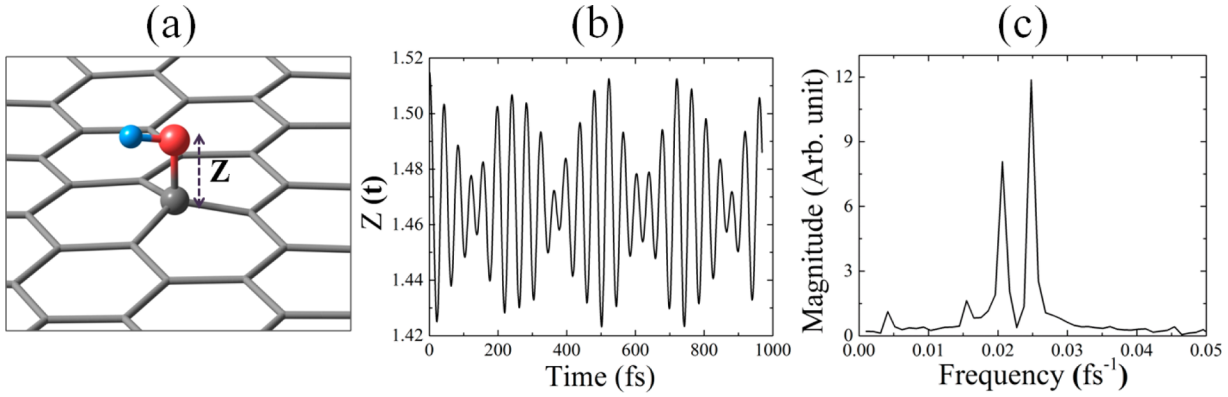

Figure 2. (a) Optimized geometry for OH-adsorbed graphene. (b) Changes in the C−O bond length (Z) with time in the AIMD calculation. (c) Fourier transformation of $Z(t)$. Atomic symbols for panel a are the same as those used in Figure 1.

respectively, in the case of an isolated neutral radical OH. On the other hand, when it is in the TS configuration (Figure 1b), the charges on O and H are −1.4 and +1, respectively, and this charge gain of 0.4 by O can be attributed to the anionic state of OH. To calculate the energy barrier (ΔE) to the desorption of OH, we calculated the MEP by calculating six intermediate steps between the initial and final configurations. The value of ΔE is found to be 0.87 eV. Later, we use the Arrhenius-type equation $k = \nu \exp(-\Delta E/k_B T)$ to evaluate the reaction rate[25] and show that the resonantly oscillating E-field provides the energy required to overcome ΔE and to initiate the otherwise unfavorable reaction.

We now determine the resonant frequency (RF) of the C−O bond of the adsorbed OH in the model system shown in Figure 2a. To characterize the vibration and to single out the C−O vibration embedded in several phonon modes, we performed the AIMD simulations with various initial conditions, and followed the length of the C−O bond in real time. Figure 2b shows the C−O bond length, denoted by $Z(t)$, after the geometry was released from an initially perturbed configuration where the OH is shifted upward by 0.1 Å from the equilibrium position. To extract the RF of the vibration, we performed fast Fourier transform (FFT) analysis for the time series $Z(t)$ shown in Figure 2c. We calculated 3000 AIMD steps with a time step of 0.968 fs, and Figure 2b shows only some of them. There are two prominent peaks in Figure 2c: 0.021 and 0.025 fs^{-1}. We tested the AIMD calculations with both frequencies and found that, while both can lead to the amplification of the C−O bond length, the OH adsorbates responded more sharply to the higher one (0.025 fs^{-1}). In reality, because of the large anharmonicity and softening along the direction of C−O bond elongation, the desorption reaction cannot be fully resonated by a single frequency. Instead, our real-time AIMD simulation suggests that an oscillating E-field with a frequency around 0.02 fs^{-1} is useful for the substantial activation of the C−O bond.

We also calculated the phonon spectrum using the density functional perturbation theory, as presented in Figure S1 in the Supporting Information. We found a phonon mode which mostly originates from the C−O vibration. From the calculations of total and partial phonon density of states as given in Figure S1, the RF is found to be 0.024 fs^{-1}, in close agreement with the RF calculated from the FFT analysis. However, it should be noted that the phonons are normal modes of the vibration, which are not necessarily localized in a particular bond such as C−O. The localized bond vibration, possibly represented by linear combinations of a few phonon modes, is a more relevant quantity for this study. That was the reason why we traced the real-time vibration of C−O. Using the obtained vibration frequency, we deduced the rate of reaction from the Arrhenius-type equation. With the energy barrier obtained from NEB calculation ($\Delta E \approx 0.87$ eV in Figure 1b), the desorption rate at room temperature $k = \nu \exp(-\Delta E/k_B T)$ is found to be 4.08×10^{-17} fs^{-1}.

We now show that, under an oscillating RF E-field, C−O bond length associated with the OH is monotonically increased, leading to the detachment of OH from the surface. For a clear comparison we also performed the AIMD simulations with a few off-resonant frequencies (ORFs). Initially, the system in the ground state was subjected to an E-field of RF 0.025 fs^{-1}, i.e., Z = 1.47 Å at 0.0 ps, as sketched in the left panel of Figure 3a, and the system arrives at the detached configuration of OH at around 1 ps, as depicted in the right panel of Figure 3a. The direction of the E-field is set to be perpendicular to the graphene plane, and the time series of C−O bond lengths ($Z(t)$) is shown in Figure 3b. After removal, OH wanders over the surface of the graphene. In our AIMD runs, the maximum value of Z attained is 7.72 Å at 2.19 ps. It is noted that the OH approaches the graphene plane with a minimum value of Z = 1.19 Å at 2.72 ps in Figure 3b. Nevertheless, due to its increased kinetic energy, this did not lead to the formation of a C−O bond.

As presented in Figure 3b, the time-evolution of Z was also calculated with two ORFs: one is lower (0.005 fs^{-1}) and the other is higher (0.045 fs^{-1}) than the RF. The intensity of the E-field used is the same as that of the E-field of RF. With these frequencies out of the resonance, the elongation of C−O bond length is negligible. Throughout the simulated time window, OH remains mostly intact on the graphene. The maximum value of Z attained is 1.78 Å at 0.48 ps and 1.70 Å at 1.34 ps in the case of 0.005 and 0.045 fs^{-1} frequencies, respectively.

In these simulations for the resonance phenomena, the most important factor is whether the frequency of the external field is fitted to the vibration mode or not. The strength of the E-field does not much matter, as confirmed by previous studies.[23] In Figure 3c, we plotted $Z(t)$ with a frequency close to the RF (ν = 0.023 fs^{-1}) but with a different E-field strength: E = 0.025 V/Å. The wavy pattern of the $Z(t)$, shown in the inset of Figure 3c, clearly indicates the monotonic increase of the amplitude, which is the characteristic of the resonance. The OH was obviously detached from the surface at around 1.0 ps. In a realistic situation, if a field is applied to a bulk material sample, there must be an amount of screening over the material's

DOI: 10.1021/acs.jpclett.5b02420
J. Phys. Chem. Lett. 2015, 6, 5094−5099

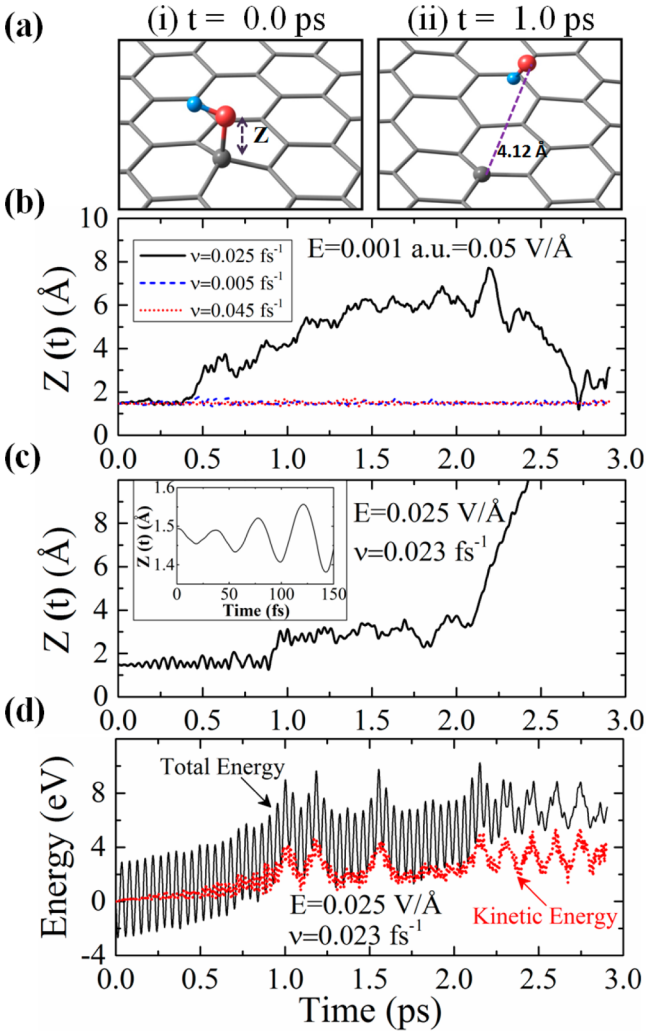

Figure 3. AIMD calculations with an oscillating E-field. (a) Configurations of the initial equilibrium system and that with the detached OH. (b) The bond length (Z) with elapsed time with the resonant (0.025 fs^{-1}) and off-resonant frequencies (0.025 fs^{-1} and 0.025 fs^{-1}) and with E = 0.05 V/Å. (c) The bond length (Z) with elapsed time with the resonant frequency of 0.023 fs^{-1} and with E = 0.025 V/Å. (d) Total and kinetic energy of the system with elapsed time for the case in panel c. Atomic symbols for panel a are the same as those used in Figure 1. The geometry in part ii of panel a is taken at 1.0 ps for the resonant case in panel b.

thickness; thus, we can hardly estimate the exact magnitude of the field acting on the nanomaterial's surface. Nevertheless, the frequency of the field can be critically effective. Compared to the negligible desorption rate (4.08×10^{-17} fs^{-1}) estimated from the Arrhenius-type equation in the previous paragraph, the resonating E-field contributed to the very fast desorption of OH roughly within 1.0 ps. It is also worth mentioning that this type of resonant excitation was localized on the C−OH bond without causing defects to the graphene.

The time evolution of the relative total energy (TE), with respect to the TE of the initial equilibrium configuration, and the kinetic energy (KE) of the system are presented in Figure 3d. As the external E-field amplified the C−OH bond vibration, both the TE and KE of the system increased up to 1.0 ps. It is noticeable that, besides the short-time fluctuation, the TE and KE saturate after 1.0 ps. This means that after the full detachment of OH, the oscillating E-field did not effectively increase the energy of the system. The increased KE of the system up to 1.0 ps are sufficient to overcome the static energy barrier (ΔE) of 0.87 eV. In this simulation, we did not use the thermostat; thus, the temperature was not defined in the simulation. In the conventional AIMD simulation, the atomic speeds are scaled with the defined temperature through a thermostat. However, it should be noted that such a scaling of the kinetic energy is irrelevant to this study. The activated particular bond, as a result of the resonance with the external field, is out of the thermal equilibrium. Besides the selected bond that was resonantly excited, the other part of the structure did not deviate much from the equilibrium structure. This suggests that, in a realistic situation, the work done by the resonating E-field selectively heats the local bond out of the thermal equilibrium, while the other part mostly remained in thermal equilibrium.

An oscillating resonant E-field can be used to open new paths for kinetically limited chemical processes by exciting specific bonds in the reaction. To demonstrate this, we explore a possible path for the production of amine-enriched functional groups on common GO derivatives. This amine-enriched surface is desired owing to its potential applications in areas such as waste stream treatment,[26] the preparation of antifouling surfaces,[27] and cell-resistant systems.[28] As a simplified model for GO, we first consider a graphene surface with a single OH and an ammonia (NH_3) molecule nearby, as indicated by IS in Figure 4a. The TS configuration (inset of Figure 4b) shows that OH is detached from the carbon plane and captures the hydrogen from NH_3, forming a desorbed water (H_2O) molecule, leaving behind an amine (NH_2) functional group. A barrier (ΔE) of 0.88 eV is calculated as a result of NEB calculations. The final product of amine-functionalized graphene with the desorbed H_2O is shown in Figure 4c, as indicated by FS. A similar amination process of the graphene with an epoxy functional group is provided in Figure S2.

Because of the limitation imposed by the computation cost, our MD simulation was restricted to a few picoseconds, which seems to be far too short for the complete surveying of all possible configurations. Nevertheless, even with this computational limitation, the resonance-induced activation of the reaction can be explained by plotting the total energy variation with respect to time, as show in Figure 4d. Upon the presence of the resonant E-field, the energy of the system increased by accumulating the kinetic energy of the resonantly vibrating part. At around 0.83 ps, the accumulated kinetic energy exceeded the energy barrier. The configuration of the system at 0.83 ps is given in Figure 4e: the detached OH is in close proximity to the elongated H of the NH_3. Because of the limited cross-section between the reacting species within the simulated time window, the final aminated structure was not identified in the AIMD simulation. However, we conjecture that such an activated structure, as depicted in Figure 4e, can lead to the final structure without energy barrier. It is thought that, for a realistic reaction, a longer time simulation is necessary over a few tens or hundreds of picoseconds. Additionally, in a practical situation, the condensed phase of the reactant can increase the chance of collision between the generated reactive species.

In summary, using the first-principles calculations, we investigated the effect of a resonantly oscillating E-field on adsorbed functional groups on graphene. To perform the AIMD simulation with the oscillating E-field, we implemented the oscillating bias potential in the Kohn−Sham Hamiltonian in the Quantum ESPRESSO code. As an example, we considered

DOI: 10.1021/acs.jpclett.5b02420
J. Phys. Chem. Lett. 2015, 6, 5094−5099

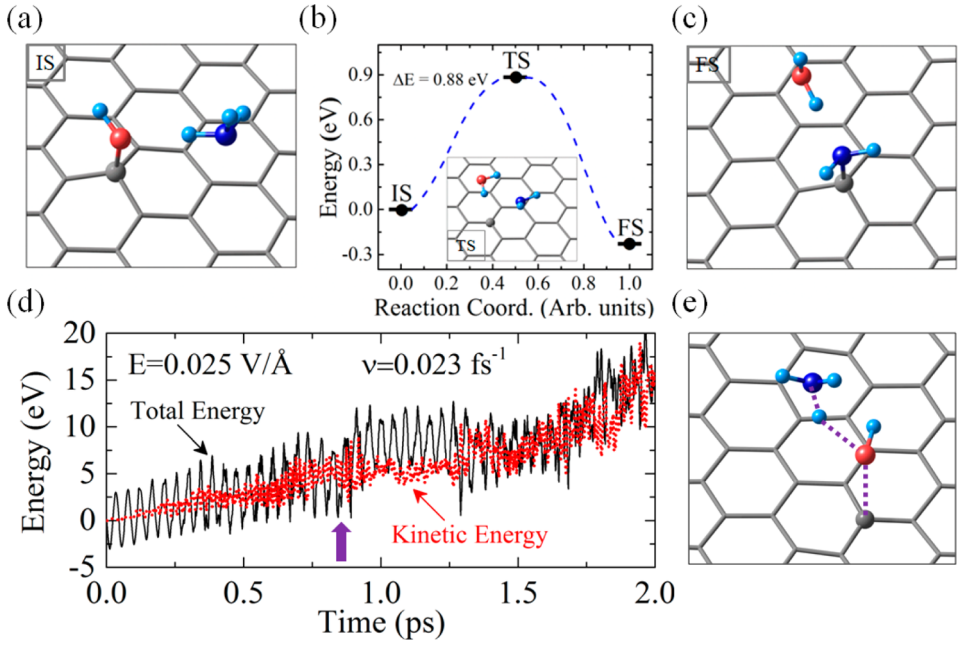

Figure 4. Path for enriching amine functional groups on graphene. The initial state (IS), transition state (TS), and final state (FS) configurations for the amination process of the OH-adsorbed graphene are represented by panel a, the inset of panels b, and panel c, respectively. (d) Change of the total and kinetic energy of the system with elapsed time. (e) The configuration of the system at 0.83 ps during AIMD simulation. Dark blue balls indicate N atoms while all other atomic symbols and the labels for the configurations are the same as those used in Figure 1.

OH adsorbed on graphene. A tuned E-field of frequency 0.025 fs^{-1} led to a rapid elongation of the C−O bond associated with the resonant vibration of OH. As a consequence, the system is able to overcome the potential energy barrier of 0.87 eV. We suggest that this method opens the possibility of obtaining custom-tailored surfaces with atomic-size controlled chemistry. As an example, we considered the resonant activation of oxygen species on GO in the presence of ammonia, which may lead to amine functionalization of the graphene surface.

■ ASSOCIATED CONTENT

Supporting Information

The Supporting Information is available free of charge on the ACS Publications website at DOI: 10.1021/acs.jpclett.5b02420.

The total PhDOS of the OH adsorbed graphene system and the partial PhDOS projected onto O atom (Figure S1) and NEB calculations along with the IS, TS, and FS configurations for the amination process from the epoxy functional group on graphene (Figure S2) (PDF)

■ AUTHOR INFORMATION

Corresponding Author

*E-mail: noejung@unist.ac.kr.

Notes

The authors declare no competing financial interest.

■ ACKNOWLEDGMENTS

This work is supported by the Institute for Basic Science (IBS-R019-D1).

■ REFERENCES

(1) Sodhi, R. N. Application of Surface Analytical and Modification Techniques to Biomaterial Research. *J. Electron Spectrosc. Relat. Phenom.* **1996**, *81*, 269−284.

(2) Wan, Q.; Tian, J.; Liu, M.; Zeng, G.; Li, Z.; Wang, K.; Zhang, Q.; Deng, F.; Zhang, X.; Wei, Y. Mussel Inspired Preparation of Highly Dispersible and Biocompatible Carbon Nanotubes. *RSC Adv.* **2015**, *5*, 25329−25336.

(3) Huang, G.; Zhang, C.; Li, S.; Khemtong, C.; Yang, S.-G.; Tian, R.; Minna, J. D.; Brown, K. C.; Gao, J. A Novel Strategy for Surface Modification of Superparamagnetic Iron Oxide Nanoparticles for Lung Cancer Imaging. *J. Mater. Chem.* **2009**, *19*, 6367−6372.

(4) Jing, L.; Zhou, W.; Tian, G.; Fu, H. Surface Tuning for Oxide-Based Nanomaterials as Efficient Photocatalysts. *Chem. Soc. Rev.* **2013**, *42*, 9509−9549.

(5) Hong, J.-Y.; Sohn, E.-H.; Park, S.; Park, H. S. Highly-Efficient and Recyclable Oil Absorbing Performance of Functionalized Graphene Aerogel. *Chem. Eng. J.* **2015**, *269*, 229−235.

(6) Saengdee, P.; Chaisriratanakul, W.; Bunjongpru, W.; Sripumkhai, W.; Srisuwan, A.; Jeamsaksiri, W.; Hruanun, C.; Poyai, A.; Promptmas, C. Surface Modification of Silicon Dioxide, Silicon Nitride and Titanium Oxynitride for Lactate Dehydrogenase Immobilization. *Biosens. Bioelectron.* **2015**, *67*, 134−138.

(7) Bigerelle, M.; Anselme, K.; Noël, B.; Ruderman, I.; Hardouin, P.; Iost, A. Improvement in the Morphology of Ti-Based Surfaces: a New Process to Increase in Vitro Human Osteoblast Response. *Biomaterials* **2002**, *23*, 1563−1577.

(8) Anselme, K.; Bigerelle, M. Topography Effects of Pure Titanium Substrates on Human Osteoblast Long-Term Adhesion. *Acta Biomater.* **2005**, *1*, 211−222.

(9) Chiavari, C.; Balbo, A.; Bernardi, E.; Martini, C.; Zanotto, F.; Vassura, I.; Bignozzi, M. C.; Monticelli, C. Organosilane Coatings Applied on Bronze: Influence of UV Radiation and Thermal Cycles on the Protectiveness. *Prog. Org. Coat.* **2015**, *82*, 91−100.

(10) Stuckert, E. P.; Fisher, E. R. Ar/O_2 and H+O Plasma Surface Modification of SnO_2 Nanomaterials to Increase Surface Oxidation. *Sens. Actuators, B* **2015**, *208*, 379−388.

(11) Jia, X.; Herrera-Alonso, M.; McCarthy, T. J. Nylon Surface Modification. Part 1. Targeting the Amide Groups for Selective Introduction of Reactive Functionalities. *Polymer* **2006**, *47*, 4916−4924 and references therein..

DOI: 10.1021/acs.jpclett.5b02420
J. Phys. Chem. Lett. 2015, 6, 5094−5099

(12) Jiang, Z.; Jiang, Z.-J. Plasma Techniques for the Fabrication of Polymer Electrolyte Membranes for Fuel Cells. *J. Membr. Sci.* **2014**, *456*, 85−106.
(13) Ginn, B. T.; Steinbock, O. Polymer Surface Modification Using Microwave-Oven-Generated Plasma. *Langmuir* **2003**, *19*, 8117−8118.
(14) Tian, Y.; Chen, C.; Li, S.; Huo, Q. Research Progress on Laser Surface Modification of Titanium Alloys. *Appl. Surf. Sci.* **2005**, *242*, 177−184.
(15) Garcia, B. B.; Candelaria, S. L.; Cao, G. Nitrogenated Porous Carbon Electrodes for Supercapacitors. *J. Mater. Sci.* **2012**, *47*, 5996−6004.
(16) Guo, Y.; Xu, K.; Wu, C.; Zhao, J.; Xie, Y. Surface Chemical-Modification for Engineering the Intrinsic Physical Properties of Inorganic Two-Dimensional Nanomaterials. *Chem. Soc. Rev.* **2015**, *44*, 637.
(17) Giannozzi, P.; Baroni, S.; Bonini, N.; Calandra, M.; Car, R.; Cavazzoni, C.; Ceresoli, D.; Chiarotti, G. L.; Cococcioni, M.; Dabo, I. QUANTUM ESPRESSO: A Modular and Open-Source Software Project for Quantum Simulations of Materials. *J. Phys: Condens. Matter* **2009**, *21*, 395502.
(18) Perdew, J. P.; Wang, Y. Accurate and Simple Analytic Representation of the Electron-Gas Correlation Energy. *Phys. Rev. B: Condens. Matter Mater. Phys.* **1992**, *45*, 13244−13249.
(19) Hamann, D. R.; Schlüter, M.; Chiang, C. Norm-Conserving Pseudopotentials. *Phys. Rev. Lett.* **1979**, *43*, 1494−1497.
(20) Troullier, N.; Martins, J. L. Efficient Pseudopotentials for Plane-Wave Calculations. *Phys. Rev. B: Condens. Matter Mater. Phys.* **1991**, *43*, 1993−2006.
(21) Henkelman, G.; Jónsson, H. A Dimer Method for Finding Saddle Points on High Dimensional Potential Surfaces using only First Derivatives. *J. Chem. Phys.* **1999**, *111*, 7010−7022.
(22) Weinan, E.; Ren, W.; Vanden-Eijnden, E. String Method for the Study of Rare Events. *Phys. Rev. B: Condens. Matter Mater. Phys.* **2002**, *66*, 052301.
(23) Miyamoto, Y.; Zhang, H.; Miyazaki, T.; Rubio, A. Modifying the Interlayer Interaction in Layered Materials with an Intense IR Laser. *Phys. Rev. Lett.* **2015**, *114*, 116102 and references therein.
(24) Bader, R. *Atoms in Molecules: A Quantum Theory*; Oxford University Press: New York, 1990.
(25) Laidler, K. J. The Development of the Arrhenius Equation. *J. Chem. Educ.* **1984**, *61*, 494.
(26) Deng, S.; Bai; Chen, J. P. Aminated Polyacrylonitrile Fibers for Lead and Copper Removal. *Langmuir* **2003**, *19*, 5058−5064.
(27) Dhamodharan, R.; McCarthy, T. J. Adsorption of Alginic Acid and Chondroitin Sulfate-A to Amine Functionality Introduced on Polychlorotrifluoroethylene and Glass Surfaces. *Macromolecules* **1999**, *32*, 4106−4112.
(28) Morra, M.; Cassinelli, C. Surface Studies on a Model Cell-Resistant System. *Langmuir* **1999**, *15*, 4658−4663.

DOI: 10.1021/acs.jpclett.5b02420
J. Phys. Chem. Lett. 2015, 6, 5094−5099